PHYSICAL REVIEW D **79,** 115022 (2009)

Charged Higgs phenomenology in the lepton-specific two Higgs doublet model

Heather E. Logan* and Deanna MacLennan

Ottawa-Carleton Institute for Physics, Carleton University, Ottawa K1S 5B6 Canada

(Received 7 April 2009; published 25 June 2009)

We study the ''lepton-specific'' two Higgs doublet model, in which one doublet Φ_ℓ gives mass to charged leptons and the other Φ_q gives mass to both up- and down-type quarks. We examine the existing experimental constraints on the charged Higgs boson mass and the parameter $\tan\beta \equiv \langle\Phi_q^0\rangle/\langle\Phi_\ell^0\rangle$. The most stringent constraints come from LEP-II direct searches and lepton flavor universality in τ decays. The former yields $M_{H^\pm} \geq 92.0$ GeV; the latter yields two allowed regions $0.61\tan\beta$ GeV $\leq M_{H^\pm} \leq 0.73\tan\beta$ GeV or $M_{H^\pm} \geq 1.4\tan\beta$ GeV, and excludes parameter regions beyond the LEP-II bound for $\tan\beta \gtrsim 65$. We present the charged Higgs decay branching fractions and discuss prospects for charged Higgs discovery at the LHC in this model.

DOI: 10.1103/PhysRevD.79.115022 PACS numbers: 14.80.Cp

I. INTRODUCTION

While the standard model (SM) of electroweak interactions has been rigorously tested over the past two decades, the dynamics of electroweak symmetry breaking have yet to be probed directly. This leaves open the possibility of an extended Higgs sector more complicated than the single SU(2) doublet present in the SM.

Models with two Higgs doublets (2HDMs) have been studied extensively. In particular, the Type-II 2HDM [1–4], in which one doublet generates the masses of up-type quarks, while the other generates the masses of down-type quarks and charged leptons, arises naturally in supersymmetric models; its collider phenomenology has received much attention. The Type-I 2HDM [5,6], in which one doublet generates the masses of all quarks and leptons, while the other contributes only to the W and Z boson masses, has also been widely considered, particularly in the context of indirect constraints. Other patterns of couplings of two Higgs doublets to SM fermions have been introduced [7–9], but their phenomenology has not been extensively explored.

In this paper we study the ''lepton-specific'' two Higgs doublet model,[1] in which one doublet Φ_ℓ generates the masses of the charged leptons, while the second doublet Φ_q generates the masses of both up- and down-type quarks. This coupling structure was first introduced in Refs. [7–9], and initial studies of the Higgs boson couplings and their detection prospects at the CERN Large Electron Positron (LEP) collider were made in Ref. [13]. Further studies of the couplings, decays, and phenomenology at the CERN Large Hadron Collider (LHC) of mainly the neutral Higgs bosons in this model have been made in Refs. [10–12,14–16]. This doublet structure was also introduced in Ref. [17] [along with additional SU(2) singlet scalars] in order to avoid the stringent constraints on the charged Higgs mass from $b \to s\gamma$ [18] that arise in the usual Type-II 2HDM.

We focus here on the charged Higgs boson $H^\pm$. We study the existing experimental constraints on the charged Higgs mass from direct searches as well as indirect constraints on the mass and couplings from virtual charged Higgs exchange in both tree-level and one-loop processes. Because of the structure of the Yukawa Lagrangian, couplings of $H^\pm$ to leptons are enhanced by a factor of $\tan\beta \equiv \langle\Phi_q^0\rangle/\langle\Phi_\ell^0\rangle$, while couplings of $H^\pm$ to quarks contain a factor of $\cot\beta$. This leads to different indirect constraints and charged Higgs decay branching fractions than in the usual Type-I or II 2HDMs.

This paper is organized as follows: In Sec. II, we outline the model and present the relevant Feynman rules for the couplings of the charged Higgs to fermions. In Sec. III, we present the constraints on the charged Higgs sector from direct searches at LEP II as well as indirect constraints from virtual charged Higgs exchange. The most stringent indirect constraint comes from μ–e universality in τ decays. We also review the charged Higgs effects in muon and τ decay distributions, B^+ and D_s^+ leptonic decays, $b \to c\tau\nu$, $B_{(s)} \to \ell^+\ell^-$, and $b \to s\gamma$. In Sec. IV, we plot the decay branching fractions of $H^\pm$ as a function of the charged Higgs mass for various values of $\tan\beta$ and compare them to those in the usual Type-II 2HDM. We finish in Sec. V with a discussion of charged Higgs search prospects at the LHC and a summary of our conclusions.

II. THE MODEL

We begin with two complex SU(2)-doublet fields Φ_q and Φ_ℓ, with

$$\Phi_i = \begin{pmatrix} \phi_i^+ \\ \frac{1}{\sqrt{2}}(\phi_i^{0,r} + v_i + i\phi_i^{0,i}) \end{pmatrix}, \qquad i = q, \ell. \quad (1)$$

The structure of the Yukawa Lagrangian that characterizes this model is enforced by imposing a discrete symmetry

*logan@physics.carleton.ca

[1] In the literature, this scenario has also been referred to as Model IIA [7,8], Model I′ [9], the leptonic Higgs [10], the Type-X 2HDM [11], and the leptophilic 2HDM [12].

under which Φ_ℓ and the right-handed leptons transform as

$$\Phi_\ell \to -\Phi_\ell, \qquad e_{Ri} \to -e_{Ri}, \tag{2}$$

while all other fields remain unchanged. The resulting Yukawa Lagrangian is

$$\mathcal{L}_{\rm Yuk} = -\sum_{i,j=1}^{3} [y^u_{ij}\bar{u}_{Ri}\tilde{\Phi}_q^\dagger Q_{Lj} + y^d_{ij}\bar{d}_{Ri}\Phi_q^\dagger Q_{Lj} + y^\ell_{ij}\bar{e}_{Ri}\Phi_\ell^\dagger L_{Lj}] + \text{H.c.}, \tag{3}$$

where i, j are generation indices, $y^{u,d,\ell}_{ij}$ are the Yukawa coupling matrices, the left-handed quark and lepton doublets are

$$L_{Li} = \begin{pmatrix} \nu_{Li} \\ e_{Li} \end{pmatrix}, \qquad Q_{Li} = \begin{pmatrix} u_{Li} \\ d_{Li} \end{pmatrix}, \tag{4}$$

and the conjugate Higgs doublet is given by

$$\tilde{\Phi}_q \equiv i\sigma_2\Phi_q^* = \begin{pmatrix} \frac{1}{\sqrt{2}}(\phi_q^{0,r} + v_q - i\phi_q^{0,i}) \\ -\phi_q^- \end{pmatrix}. \tag{5}$$

The charged states ϕ_q^+ and ϕ_ℓ^+ mix to form the charged Goldstone boson and a single physical charged Higgs state

$$H^+ = -\phi_\ell^+ \sin\beta + \phi_q^+ \cos\beta, \tag{6}$$

where we define $\tan\beta = v_q/v_\ell$. We also have $\sqrt{v_q^2 + v_\ell^2} = v_{\rm SM} = 2M_W/g \simeq 246$ GeV, where M_W is the W boson mass and g is the SU(2) gauge coupling.

The Feynman rules for charged Higgs boson couplings to fermions are given as follows, with all particles incoming[2]:

$$\begin{aligned} H^+\bar{u}_i d_j &: \frac{ig}{\sqrt{2}M_W} V_{ij}\cot\beta(m_{u_i}P_L - m_{d_j}P_R), \\ H^+\bar{\nu}_{e_k} e_k &: \frac{ig}{\sqrt{2}M_W}\tan\beta m_{e_k}P_R. \end{aligned} \tag{9}$$

[2]For comparison, the corresponding couplings in the Type-I 2HDM are [19]

$$\begin{aligned} H^+\bar{u}_i d_j &: \frac{ig}{\sqrt{2}M_W} V_{ij}\cot\beta(m_{u_i}P_L - m_{d_j}P_R), \\ H^+\bar{\nu}_{e_k} e_k &: -\frac{ig}{\sqrt{2}M_W}\cot\beta m_{e_k}P_R, \end{aligned} \tag{7}$$

with $\tan\beta = v_2/v_1$, where v_2 is the vacuum expectation value of the Higgs field that couples to fermions; the other doublet is decoupled from fermions. In the Type-II 2HDM the couplings are [19]

$$\begin{aligned} H^+\bar{u}_i d_j &: \frac{ig}{\sqrt{2}M_W} V_{ij}(\cot\beta m_{u_i}P_L + \tan\beta m_{d_j}P_R), \\ H^+\bar{\nu}_{e_k} e_k &: \frac{ig}{\sqrt{2}M_W}\tan\beta m_{e_k}P_R, \end{aligned} \tag{8}$$

again with $\tan\beta = v_2/v_1$; this time v_1 (v_2) is the vacuum expectation value of the doublet that couples to down-type quarks and charged leptons (up-type quarks).

Here, V_{ij} is the relevant Cabibbo-Kobayashi-Maskawa matrix element and $P_{L,R} \equiv (1 \mp \gamma^5)/2$ are the left- and right-handed projection operators.

Note that the $H^+\bar{\nu}\ell$ couplings are enhanced at large $\tan\beta$, while the $H^+\bar{u}d$ couplings are suppressed. This enhancement of the lepton couplings is due to the m_ℓ/v_ℓ dependence of the lepton Yukawa couplings

$$y_\ell = \frac{\sqrt{2}m_\ell}{v_\ell} = \frac{\sqrt{2}m_\ell}{v_{\rm SM}\cos\beta}. \tag{10}$$

The maximum value of $\tan\beta$ is limited by the requirement that the τ Yukawa coupling remain perturbative,

$$y_\tau = \frac{\sqrt{2}m_\tau}{v_{\rm SM}\cos\beta} \lesssim 4\pi. \tag{11}$$

This leads to an upper bound on $\tan\beta$ of

$$\tan\beta \lesssim 1200. \tag{12}$$

In our numerical results we will consider values of $\tan\beta$ up to 100 or 200, corresponding to y_τ values of about 1 or 2, respectively.

III. EXPERIMENTAL CONSTRAINTS

A. LEP-II direct search

The four LEP collaborations have presented combined limits [20] for $e^+e^- \to H^+H^-$ with $H^+ \to \tau\nu$ or $c\bar{s}$, assuming that the branching ratios of these two decays add to 1. The 95% confidence level (C.L.) limits range from $M_{H^\pm} \geq 78.6$ GeV to 89.6 GeV; the strongest limit is reached for BR$(H^+ \to \tau\nu) = 1$. Separately, the OPAL Collaboration presented a charged Higgs search in the $\tau\nu\tau\nu$ channel alone assuming BR$(H^+ \to \tau\nu) = 1$, which excludes $M_{H^\pm}$ values below 92.0 GeV at 95% C.L. [21].

In this paper we are interested in $\tan\beta$ values greater than a few. In this case, as we will show in Sec. IV, the branching ratio of $H^+ \to \tau\nu$ is very close to 1 for charged Higgs masses in the region of the LEP-II limit. We therefore take the more stringent OPAL limit [21]

$$M_{H^\pm} \geq 92.0 \text{ GeV}. \tag{13}$$

B. Lepton universality in τ decays

The decays $\tau \to \mu\bar{\nu}_\mu\nu_\tau$, $\tau \to e\bar{\nu}_e\nu_\tau$, and $\mu \to e\bar{\nu}_e\nu_\mu$ proceed at tree level in the SM through virtual W exchange. In models with two Higgs doublets they also receive a contribution from tree-level charged Higgs exchange. The tree-level partial width for these decays in the lepton-specific 2HDM is identical to that in the Type-II 2HDM [22,23],

$$\Gamma(L \to \ell \bar{\nu}_\ell \nu_L) = \frac{G_F^2 m_L^5}{192\pi^3}\left[\left(1 + \frac{1}{4} m_\ell^2 m_L^2 \frac{\tan^4\beta}{M_{H^\pm}^4}\right) f(m_\ell^2/m_L^2) - 2m_\ell^2 \frac{\tan^2\beta}{M_{H^\pm}^2} g(m_\ell^2/m_L^2)\right], \tag{14}$$

where here L denotes the initial lepton, ℓ denotes the final-state charged lepton, and the phase space factors f and g are given by [23]

$$\begin{aligned} f(x) &= 1 - 8x + 8x^3 - x^4 - 12x^2 \ln x, \\ g(x) &= 1 + 9x - 9x^2 - x^3 + 6x(1 + x)\ln x. \end{aligned} \tag{15}$$

The two terms in the parentheses in Eq. (14) come from the square of the usual SM $W^\pm$ exchange diagram and the square of the charged Higgs exchange diagram, respectively. The remaining term is the (destructive) interference between the $W^\pm$ diagram and the charged Higgs diagram, which requires a helicity flip of the final-state lepton ℓ yielding an extra suppression factor m_ℓ/m_L and a different phase space factor. Because of the lepton mass dependence, the effect of the charged Higgs exchange will be largest in $\tau \to \mu\bar{\nu}\nu$.

Additional 2HDM corrections to charged lepton decay arise from one-loop diagrams involving charged and neutral Higgs bosons contributing to the $L\nu_L W$ and $\ell\nu_\ell W$ vertices [24]. Particularly significant are the corrections to the $\tau\nu_\tau W$ vertex, because they involve two powers of the τ Yukawa coupling and are not suppressed by the charged Higgs coupling to muons or electrons. These τ vertex corrections are the same for the $\tau \to \mu\bar{\nu}\nu$ and $\tau \to e\bar{\nu}\nu$ channels. They also depend on the neutral Higgs masses and mixing angle as well as $M_{H^\pm}$ and $\tan\beta$. In the present paper we focus on the charged Higgs sector alone; we will therefore consider an observable in which the one-loop corrections to the $\tau\nu W$ vertex cancel.

The SM $W^+\ell\bar{\nu}$ couplings are generation universal and τ and muon decay suffer no helicity suppression. The $H^+\ell\bar{\nu}$ couplings, on the other hand, depend on the mass of the charged lepton involved. Therefore, tests of flavor universality in the couplings that mediate τ and muon decays are sensitive to charged Higgs contributions. The τ decay rates can be written in terms of the muon lifetime τ_μ in the standard form (see, e.g., Ref. [25])

$$\begin{aligned} \tau_\tau &= \frac{g_\mu^2}{g_\tau^2}\tau_\mu \frac{m_\mu^5}{m_\tau^5}\mathrm{BR}(\tau \to e\bar{\nu}_e\nu_\tau)\frac{f(m_e^2/m_\mu^2)r_{RC}^\mu}{f(m_e^2/m_\tau^2)r_{RC}^\tau}, \\ \tau_\tau &= \frac{g_e^2}{g_\tau^2}\tau_\mu \frac{m_\mu^5}{m_\tau^5}\mathrm{BR}(\tau \to \mu\bar{\nu}_\mu\nu_\tau)\frac{f(m_e^2/m_\mu^2)r_{RC}^\mu}{f(m_\mu^2/m_\tau^2)r_{RC}^\tau}, \end{aligned} \tag{16}$$

where r_{RC}^i are the QED radiative corrections to the SM decays. Here, any deviations from flavor universality are parameterized by effective charged current couplings g_e, g_μ, and g_τ, which are equal to 1 in the SM. Ratios of these parameters are extracted from measurements of the τ lifetime and the τ branching ratios to $e\bar{\nu}\nu$ and $\mu\bar{\nu}\nu$. The current world-average experimental values are [25]

$$\frac{g_\mu}{g_e} = 0.9999 \pm 0.0020, \qquad \frac{g_\mu}{g_\tau} = 0.9982 \pm 0.0021. \tag{17}$$

The observable g_μ/g_e comes from the ratio of the τ leptonic branching fractions. In the lepton-specific 2HDM we have at tree level,

$$\frac{g_\mu^2}{g_e^2} = \frac{1 + m_\mu^2 m_\tau^2 \tan^4\beta/4M_{H^\pm}^4 - (2m_\mu^2\tan^2\beta/M_{H^\pm}^2)g(m_\mu^2/m_\tau^2)/f(m_\mu^2/m_\tau^2)}{1 + m_e^2 m_\tau^2 \tan^4\beta/4M_{H^\pm}^4 - (2m_e^2\tan^2\beta/M_{H^\pm}^2)g(m_e^2/m_\tau^2)/f(m_e^2/m_\tau^2)}, \tag{18}$$

and one-loop 2HDM corrections to the $\tau\nu W$ vertex cancel in the ratio.[3] The square root of this ratio is plotted in Fig. 1 as a function of $M_{H^\pm}/\tan\beta$, along with the current 2σ experimental limits from Ref. [25]. Inserting the experimental results yields two allowed regions at 95% C.L.:

$$0.61\tan\beta \text{ GeV} \leq M_{H^\pm} \leq 0.73\tan\beta \text{ GeV} \quad \text{or} \quad M_{H^\pm} \geq 1.4\tan\beta \text{ GeV}. \tag{20}$$

This constraint begins to exclude parameter regions beyond the LEP-II bound when $\tan\beta \gtrsim 65$.

Measurements of τ branching fractions from the proposed SuperB high-luminosity flavor factory [26] are expected to improve the precision on g_μ/g_e to better than 0.05% [25]. In the absence of a deviation from the SM prediction, this would give an even tighter constraint on the charged Higgs mass,

$$0.64\tan\beta \text{ GeV} \leq M_{H^\pm} \leq 0.67\tan\beta \text{ GeV} \quad \text{or} \quad M_{H^\pm} \geq 3.2\tan\beta \text{ GeV (SuperB)}. \tag{21}$$

Such a constraint would exclude parameter regions beyond the LEP-II bound when $\tan\beta \gtrsim 30$.

[3] We note that the tree-level expression for the other observable,

$$\frac{g_\mu^2}{g_\tau^2} = \frac{1 + m_e^2 m_\mu^2 \tan^4\beta/4M_{H^\pm}^4 - (2m_e^2\tan^2\beta/M_{H^\pm}^2)g(m_e^2/m_\mu^2)/f(m_e^2/m_\mu^2)}{1 + m_e^2 m_\tau^2 \tan^4\beta/4M_{H^\pm}^4 - (2m_e^2\tan^2\beta/M_{H^\pm}^2)g(m_e^2/m_\tau^2)/f(m_e^2/m_\tau^2)}, \tag{19}$$

is very close to its SM value due to the m_e factors in the charged Higgs exchange terms. This observable, however, is sensitive to the one-loop corrections discussed in Ref. [24] and can be used to constrain the neutral Higgs sector of the 2HDM. Such an analysis is beyond the scope of this paper.

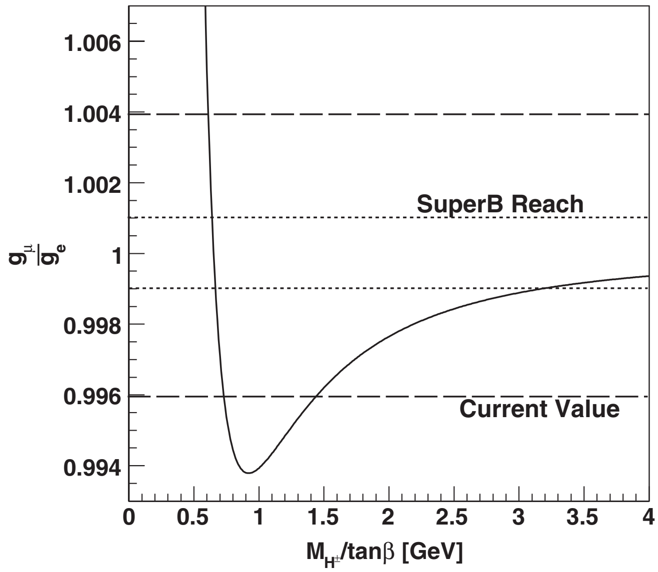

FIG. 1. Prediction for g_μ/g_e in the lepton-specific 2HDM as a function of $M_{H^\pm}/\tan\beta$ (solid line). Horizontal dashed lines indicate the current 2σ allowed range from lepton universality in τ decays (outer lines) and the future anticipated reach of SuperB (inner lines).

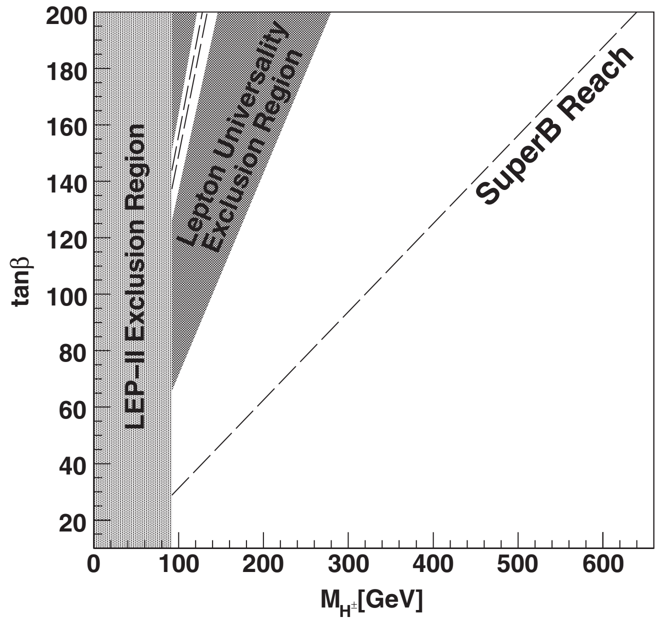

FIG. 2. Constraints on $M_{H^\pm}$ and $\tan\beta$ at 95% C.L. from LEP-II direct searches and lepton flavor universality in τ decays. The dashed lines show the anticipated reach of the SuperB experiment. Note the allowed sliver of parameter space at lower $M_{H^\pm}/\tan\beta$.

The constraints on $M_{H^\pm}$ and $\tan\beta$ due to LEP-II direct searches and flavor universality in τ decays are summarized in Fig. 2.

C. Other low-energy processes

1. Michel parameters in muon and τ decay

In the SM, muon and τ decays proceed through the left-handed vector couplings of the W boson. The H^+ exchange contribution in the lepton-specific 2HDM involves scalar couplings to right-handed charged leptons [Eq. (9)]. This different coupling structure can affect the energy and angular distribution of the daughter charged lepton in decays of polarized muons or τs. These distributions are parameterized in terms of the Michel parameters [27] ρ, ξ, δ, and η, which are defined in terms of the energy and angular distribution of the daughter charged lepton $\ell^\pm$ in the rest frame of the parent ($L^\pm$) [28]:

$$\frac{d^2\Gamma}{dx\,d\cos\theta} \propto x^2\Big\{3(1-x) + \frac{2\rho}{3}(4x-3) + 3\eta x_0(1-x)/x \pm P\xi\cos\theta\Big[1 - x + \frac{2\delta}{3}(4x-3)\Big]\Big\}. \tag{22}$$

Here, θ is the angle between the $\ell^\pm$ momentum and the parent lepton's spin, $x = 2E_\ell/m_L$, $x_0 = 2m_\ell/m_L$, P is the degree of polarization of the parent lepton, and we have neglected neutrino masses and terms higher order in m_ℓ/m_L. The SM values for the Michel parameters are $\rho = 3/4$, $\xi = 1$, $\eta = 0$, and $\delta = 3/4$.

The most general expression for the Michel parameters is given by [29]

$$\begin{aligned}
\rho &= \frac{3}{4} - \frac{3}{4}[|g^V_{RL}|^2 + |g^V_{LR}|^2 + 2|g^T_{RL}|^2 + 2|g^T_{LR}|^2 + Re(g^S_{RL}g^{T*}_{RL} + g^S_{LR}g^{T*}_{LR})],\\
\eta &= \frac{1}{2}Re[g^V_{RR}g^{S*}_{LL} + g^V_{LL}g^{S*}_{RR} + g^V_{RL}(g^{S*}_{LR} + 6g^{T*}_{LR}) + g^V_{LR}(g^{S*}_{RL} + 6g^{T*}_{RL})],\\
\xi &= 1 - \frac{1}{2}|g^S_{LR}|^2 - \frac{1}{2}|g^S_{RR}|^2 - 4|g^V_{RL}|^2 + 2|g^V_{LR}|^2 - 2|g^V_{RR}|^2 + 2|g^T_{LR}|^2 - 8|g^T_{RL}|^2 + 4Re(g^S_{LR}g^{T*}_{LR} - g^S_{RL}g^{T*}_{RL}),\\
\xi\delta &= \frac{3}{4} - \frac{3}{8}|g^S_{RR}|^2 - \frac{3}{8}|g^S_{LR}|^2 - \frac{3}{2}|g^V_{RR}|^2 - \frac{3}{4}|g^V_{RL}|^2 - \frac{3}{4}|g^V_{LR}|^2 - \frac{3}{2}|g^T_{RL}|^2 - 3|g^T_{LR}|^2 + \frac{3}{4}Re(g^S_{LR}g^{T*}_{LR} - g^S_{RL}g^{T*}_{RL}),
\end{aligned} \tag{23}$$

where the couplings are defined in terms of the most general matrix element for the charged lepton decay $L^- \to \ell^-\bar{\nu}_\ell\nu_L$ according to [30]

$$\mathcal{M} = 4\frac{G_F}{\sqrt{2}}\sum_{\gamma=S,V,T}\sum_{\alpha,\beta=R,L} g^{\gamma}_{\alpha\beta}\langle\bar{\ell}_\alpha|\Gamma^\gamma|\nu_\ell\rangle\langle\bar{\nu}_L|\Gamma_\gamma|L_\beta\rangle. \tag{24}$$

Here, $\gamma = S$, V, or T denotes scalar ($\Gamma^S = 1$), vector ($\Gamma^V = \gamma^\mu$), or tensor ($\Gamma^T = \sigma^{\mu\nu}/\sqrt{2} = i[\gamma^\mu, \gamma^\nu]/2\sqrt{2}$) interactions, respectively, and the chiralities of ℓ and L are specified by α and β, respectively.

We consider the decay $L \to \ell\bar{\nu}\nu$ where L (ℓ) is replaced by μ (e) for muon decay and by τ (μ or e) for τ decay. In the lepton-specific 2HDM, we have $g^V_{LL} = -1/4$ representing SM W boson exchange and $g^S_{RR} = m_L m_\ell \tan^2\beta/4M^2_{H^\pm}$ representing charged Higgs exchange. All other couplings $g^\gamma_{\alpha\beta}$ are zero. The Michel parameters become

$$\rho = \frac{3}{4}, \qquad \eta = -\frac{m_L m_\ell}{32}\frac{\tan^2\beta}{M^2_{H^\pm}},$$
$$\xi = 1 - \frac{m_L^2 m_\ell^2}{32}\frac{\tan^4\beta}{M^4_{H^\pm}}, \tag{25}$$
$$\xi\delta = \frac{3}{4}\left[1 - \frac{m_L^2 m_\ell^2}{32}\frac{\tan^4\beta}{M^4_{H^\pm}}\right] = \frac{3}{4}\xi.$$

The parameters ρ and δ are equal to their SM values and provide no constraints.

We summarize the constraints on $M_{H^\pm}$ and $\tan\beta$ from the Michel parameters in muon and τ decay in Table I. The strongest constraint comes from η and ξ in $\tau \to \mu\bar{\nu}\nu$, which coincidentally yield the same limit at 95% C.L.:

$$M_{H^\pm} \geq 0.34\tan\beta \text{ GeV}. \tag{26}$$

This constraint is not competitive with that from lepton flavor universality in τ decays. We note that an improvement in the 2σ lower bound on η (ξ) in $\tau \to \mu\bar{\nu}\nu$ decay to -0.010 (0.996) would be required to raise this limit to $M_{H^\pm} \geq 0.73\tan\beta$ GeV and eliminate the allowed sliver of parameter space at lower $M_{H^\pm}/\tan\beta$ values from current data on lepton universality in τ decays (see Fig. 2).

TABLE I. Current world-average values of the Michel parameters in muon and tau decay from Ref. [31] and the resulting 95% C.L. constraints on $M_{H^\pm}$ and $\tan\beta$. (No separate measurement of ξ in muon decay or of η in $\tau \to e\bar{\nu}\nu$ is quoted in Ref. [31].)

Process	Observable	Constraint
$\mu \to e\bar{\nu}\nu$	$\eta = 0.001 \pm 0.024$	$M_{H^\pm} \geq 0.006\tan\beta$ GeV
$\tau \to \mu\bar{\nu}\nu$	$\eta = 0.094 \pm 0.073$	$M_{H^\pm} \geq 0.34\tan\beta$ GeV
	$\xi = 1.030 \pm 0.059$	$M_{H^\pm} \geq 0.34\tan\beta$ GeV
$\tau \to e\bar{\nu}\nu$	$\xi = 0.994 \pm 0.040$	$M_{H^\pm} \geq 0.023\tan\beta$ GeV

2. $B^+ \to \tau^+\nu_\tau$

In the standard model, the partial width for the decay $B^+ \to \tau^+\nu_\tau$ mediated by tree-level W^+ exchange is given by

$$\Gamma_{\rm SM}(B^+ \to \tau^+\nu_\tau) = \frac{G_F^2}{8\pi} f^2_{B^+} m_{B^+} m_\tau^2 |V_{ub}|^2\left[1 - \frac{m_\tau^2}{m^2_{B^+}}\right]^2, \tag{27}$$

where m_{B^+} is the B^+ meson mass, V_{ub} is the relevant Cabibbo-Kobayashi-Maskawa matrix element, and f_{B^+} is the B^+ meson decay constant defined according to

$$if_{B^+}p_\mu = \langle 0|\bar{b}\gamma_\mu\gamma_5 u|B^+(p)\rangle. \tag{28}$$

The partial width is proportional to m_τ^2 because of helicity suppression and the term in the square brackets arises from the phase space.

In the lepton-specific 2HDM this decay receives an additional contribution from tree-level charged Higgs exchange; the total width becomes

$$\Gamma(B^+ \to \tau^+\nu_\tau) = \left[1 - \frac{m^2_{B^+}}{M^2_{H^\pm}}\right]^2 \Gamma_{\rm SM}(B^+ \to \tau^+\nu_\tau). \tag{29}$$

Here, the helicity suppression of the SM decay ensures that the charged Higgs contribution contains no additional factors of m_τ. Note that the contributions from W^+ and H^+ exchange interfere destructively. Note also that this result differs from that in the Type-II 2HDM [32],

$$\Gamma(B^+ \to \tau^+\nu_\tau) = \left[1 - \tan^2\beta\frac{m^2_{B^+}}{M^2_{H^\pm}}\right]^2 \Gamma_{\rm SM}(B^+ \to \tau^+\nu_\tau) \quad \text{(Type II 2HDM)}, \tag{30}$$

which has been used to constrain $M_{H^\pm}/\tan\beta$ in that model (for recent results see Ref. [33]). In the lepton-specific 2HDM there is no $\tan^2\beta$ enhancement of the charged Higgs contribution because while the charged Higgs coupling to leptons is proportional to $\tan\beta$, its coupling to quarks is proportional to $\cot\beta$ (Eq. (9)). Without the $\tan^2\beta$ enhancement, the contribution due to charged Higgs exchange yields only a weak bound on $M_{H^\pm}$.

The allowed charged Higgs mass values can be extracted according to[4]

$$\left[1 - \frac{m^2_{B^+}}{M^2_{H^\pm}}\right]^2 = \frac{8\pi\,{\rm BR}(B^+ \to \tau^+\nu)}{\tau_{B^+} f^2_{B^+} G_F^2 m_{B^+} m_\tau^2 |V_{ub}|^2 (1 - m_\tau^2/m^2_{B^+})^2}, \tag{31}$$

where τ_{B^+} is the B^+ lifetime. All quantities in Eq. (31) have been measured experimentally except for f_{B^+}, which

[4] The only place that other nonstandard effects could creep in to this expression is through $|V_{ub}|$, which is extracted from a SM fit to many b observables. However, we expect nonstandard effects from the lepton-specific 2HDM to be negligible in this fit because the quark Yukawa couplings are all proportional to $\cot\beta$ and thus suppressed for $\tan\beta > 1$.

can be taken from recent unquenched lattice QCD results [34]:

$$f_{B^+} = f_B = 0.216 \pm 0.022 \text{ GeV}. \tag{32}$$

The current world-average experimental value for the branching ratio $B^+ \to \tau^+ \nu_\tau$ from the BELLE and BABAR collaborations is [35]

$$\text{BR}(B^+ \to \tau^+ \nu_\tau) = (1.41^{+0.43}_{-0.42}) \times 10^{-4}. \tag{33}$$

The only other quantity in Eq. (31) with a non-negligible uncertainty is $|V_{ub}|$, for which we take the global SM fit value [31]

$$|V_{ub}| = (3.59 \pm 0.16) \times 10^{-3}. \tag{34}$$

Combining all uncertainties in quadrature we obtain[5]

$$\left[1 - \frac{m_{B^+}^2}{M_{H^\pm}^2}\right]^2 = 1.33 \pm 0.50, \tag{35}$$

which yields two allowed ranges for the charged Higgs mass at 95% C.L.:

$$\begin{aligned} 0.63 m_{B^+} \le M_{H^\pm} \le 0.80 m_{B^+} \quad \text{or} \\ M_{H^\pm} \ge 1.5 m_{B^+} = 8.1 \text{ GeV}. \end{aligned} \tag{36}$$

The lower mass window is excluded by direct searches; the remaining limit is well below the LEP-II direct search bound (Eq. (13)) and thus provides no new information.

3. $D_s^+ \to \tau^+ \nu$

The leptonic decay $D_s^+ \to \tau^+ \nu$ is completely analogous to $B^+ \to \tau^+ \nu$ with the B^+ meson ($\bar{b}u$) replaced by the D_s^+ meson ($\bar{s}c$). The current experimental value of the $D_s^+ \to \tau^+ \nu$ branching fraction is [31]

$$\text{BR}(D_s^+ \to \tau^+ \nu) = (6.6 \pm 0.6)\% \tag{37}$$

and the current unquenched lattice QCD result for f_{D_s} is [36]

$$f_{D_s} = 0.241 \pm 0.003 \text{ GeV}. \tag{38}$$

Combining all uncertainties in quadrature as in the previous section we obtain[6]

$$\left[1 - \frac{m_{D_s^+}^2}{M_{H^\pm}^2}\right]^2 = 1.37 \pm 0.13. \tag{39}$$

In particular, there is about a 40% (or 3σ) discrepancy between the SM prediction and the experimental measurement[7]; moreover, the branching fraction of $D_s^+ \to \tau^+ \nu$ is larger than the SM prediction. Because the W^+ and H^+ exchange diagrams interfere destructively in the lepton-specific 2HDM, an explanation of the discrepancy in this context would require the decay amplitude to be dominated by the charged Higgs contribution, leading at 95% C.L. to

$$M_{H^\pm} = (0.68 \pm 0.01) m_{D_s^+} = 1.34 \pm 0.02 \text{ GeV}. \tag{40}$$

This is clearly excluded by direct searches; moreover, such a light charged Higgs in this model would yield sizeable effects in $B^+ \to \tau^+ \nu$. The discrepancy thus cannot be explained in the context of the lepton-specific 2HDM.

We note here that, in the absence of a deviation from the SM prediction, the current $D_s^+ \to \tau^+ \nu$ branching fraction measurement precision would yield the allowed regions $0.69 m_{D_s^+} \le M_{H^\pm} \le 0.73 m_{D_s^+}$ or $M_{H^\pm} \ge 3.2 m_{D_s^+} = 6.2$ GeV at 95% C.L. This measurement would thus provide a weaker constraint even than $B^+ \to \tau^+ \nu$ at the current level of experimental uncertainty.

4. *Other B decays*

Other b quark decay processes have been used to constrain 2HDMs. In the lepton-specific 2HDM, however, they do not provide useful constraints at moderate to large $\tan\beta$. We discuss them briefly here.

The decay $b \to c \tau \nu$ receives a contribution from tree-level H^+ exchange [32,38,39]. However, as in the case of $B^+ \to \tau^+ \nu$, the $\tan\beta$ enhancement in the τ Yukawa coupling is cancelled by the $\cot\beta$ dependence of the quark Yukawa couplings, leading to very small charged Higgs effects, equivalent to those in the Type-II 2HDM with $\tan\beta = 1$.

The decay $B^0_{(s)} \to \ell^+ \ell^-$ receives corrections in the Type-II 2HDM enhanced by $\tan^2\beta$ [40]. In the lepton-specific 2HDM, however, there is no $\tan\beta$ enhancement, again because the $\tan\beta$ from the lepton Yukawa coupling is cancelled by $\cot\beta$ factors from the quark Yukawa couplings. The constraints from this process are thus very weak.

Finally, the charged Higgs contributions to $b \to s\gamma$ involve couplings of the charged Higgs to quarks at both vertices, yielding two factors of $\cot\beta$ from the quark Yukawa couplings in the amplitude. The prediction for this process in the lepton-specific 2HDM is in fact identical to that in the Type-I 2HDM [41]. It can be used to constrain the parameter space at small $\tan\beta$, yielding $\tan\beta \gtrsim 4$ (2) for $M_{H^\pm} = 100$ GeV (500 GeV) [12], but provides no constraints at large $\tan\beta$.[8]

D. Tevatron constraints

The Tevatron experiments have searched for charged Higgs production in top quark decays and set upper limits on the branching ratio for $t \to H^+ b$ with either $H^+ \to c\bar{s}$

[5]For the other parameters we use $\tau_{B^+} = (1.638 \pm 0.011) \times 10^{-12}$ s, $G_F = 1.166\,37(1) \times 10^{-5}$ GeV^{-2}, $m_{B^+} = 5.279\,15(31)$ GeV, and $m_\tau = 1.776\,84(17)$ GeV [31].

[6]For the remaining parameters we use $|V_{cs}| = 0.973\,34(23)$ (global SM fit value), $m_{D_s^+} = 1.968\,49(34)$ GeV, and $\tau_{D_s^+} = (500 \pm 7) \times 10^{-15}$ s [31].

[7]Ref. [37] finds a 3.8σ discrepancy after including $D_s^+ \to \mu^+ \nu$ data.

[8]It is for this reason that the lepton-specific 2HDM was used in the model of Ref. [17].

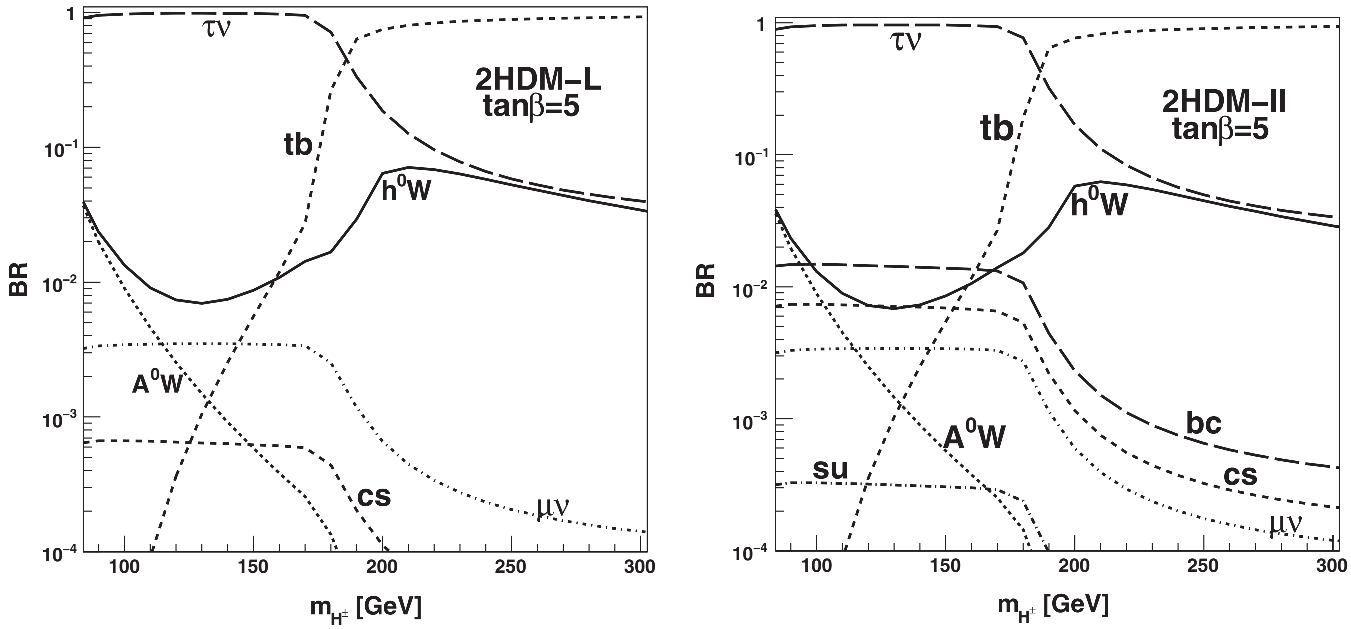

FIG. 3. Branching ratios of $H^{\pm}$ as a function of $M_{H^{\pm}}$ for $\tan\beta = 5$.

or $H^+ \to \tau\nu$ [42]. In the lepton-specific 2HDM the partial width for this top quark decay is proportional to $\cot^2\beta$, so that the channel can be important only at low $\tan\beta \sim 1$; in this parameter range the excluded regions can be taken over directly from the usual Type-II 2HDM analysis. The excluded regions lie below $\tan\beta \simeq 2$ with M_{H^+} between the LEP lower bound and about 160 GeV [42]. This parameter region is already excluded by the $b \to s\gamma$ constraint discussed in the previous section.

IV. CHARGED HIGGS BRANCHING FRACTIONS

We now present the decay branching fractions of H^+ in the lepton-specific 2HDM, which we computed using a modified version of the public FORTRAN code HDECAY [43]. HDECAY computes the charged Higgs decay branching fractions in the minimal supersymmetric standard model (MSSM), including decays to $\phi^0 W^{\pm}$ (with $\phi^0 = h^0$, H^0, or A^0) and supersymmetric particles when kine-

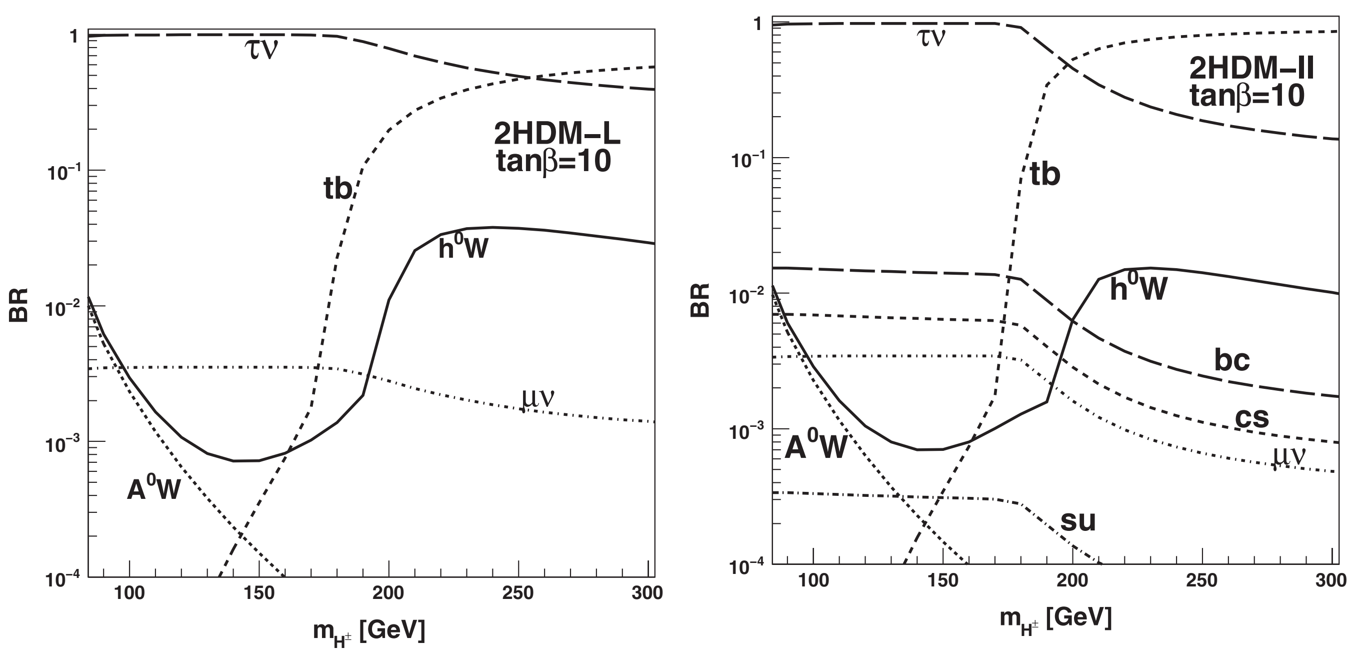

FIG. 4. Branching ratios of $H^{\pm}$ as a function of $M_{H^{\pm}}$ for $\tan\beta = 10$.

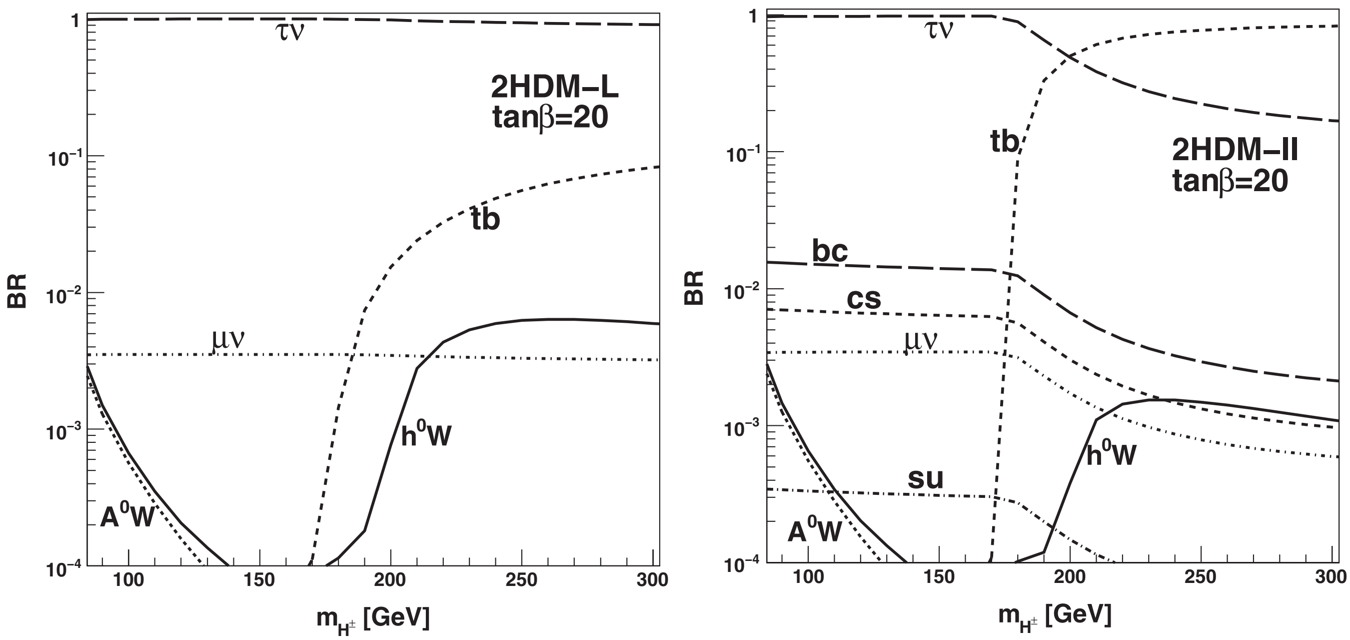

FIG. 5. Branching ratios of $H^{\pm}$ as a function of $M_{H^{\pm}}$ for $\tan\beta = 20$.

matically accessible. The Higgs sector of the MSSM has the Yukawa coupling structure of a Type-II 2HDM.

We adapt HDECAY for the lepton-specific 2HDM by modifying the charged Higgs couplings to fermions according to Eq. (9) and eliminating decays to supersymmetric particles (no explicit supersymmetric radiative corrections to charged Higgs decays are included in HDECAY). Decays to $\phi^0 W^{\pm}$ are included; these decays depend on the scalar sector of the model and their partial widths are the same in the lepton-specific 2HDM as in the Type-II model for equivalent parameter sets.

In Figs. 3–6, we show the branching ratios of $H^{\pm}$ in the lepton-specific 2HDM (2HDM-L) as a function of $M_{H^{\pm}}$ for $\tan\beta = 5$, 10, 20, and 100, respectively. For comparison we also show the branching ratios of $H^{\pm}$ in the Type-II 2HDM (2HDM-II). For the decays to $A^0 W^{\pm}$ and $h^0 W^{\pm}$, we use the A^0 and h^0 masses and the h^0–H^0 mixing angle predicted in the MSSM as a function of $M_{H^{\pm}}$ and $\tan\beta$ with all supersymmetry mass parameters set to 1 TeV.

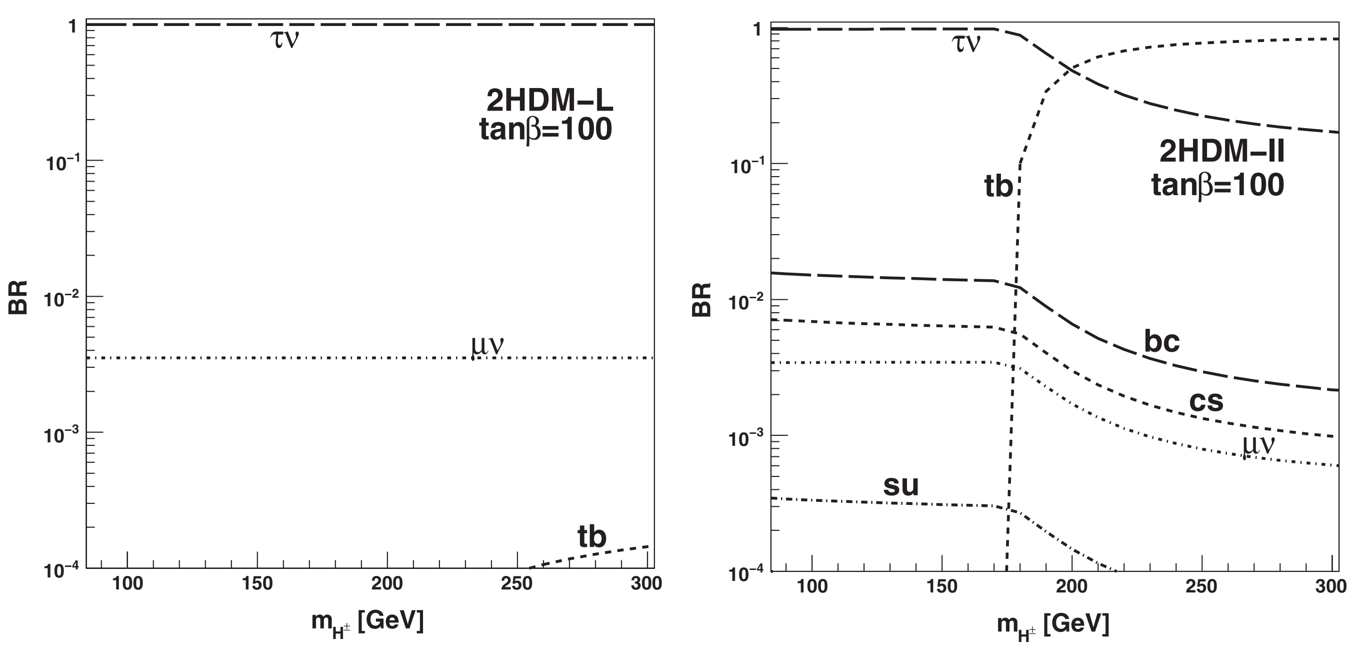

FIG. 6. Branching ratios of $H^{\pm}$ as a function of $M_{H^{\pm}}$ for $\tan\beta = 100$.

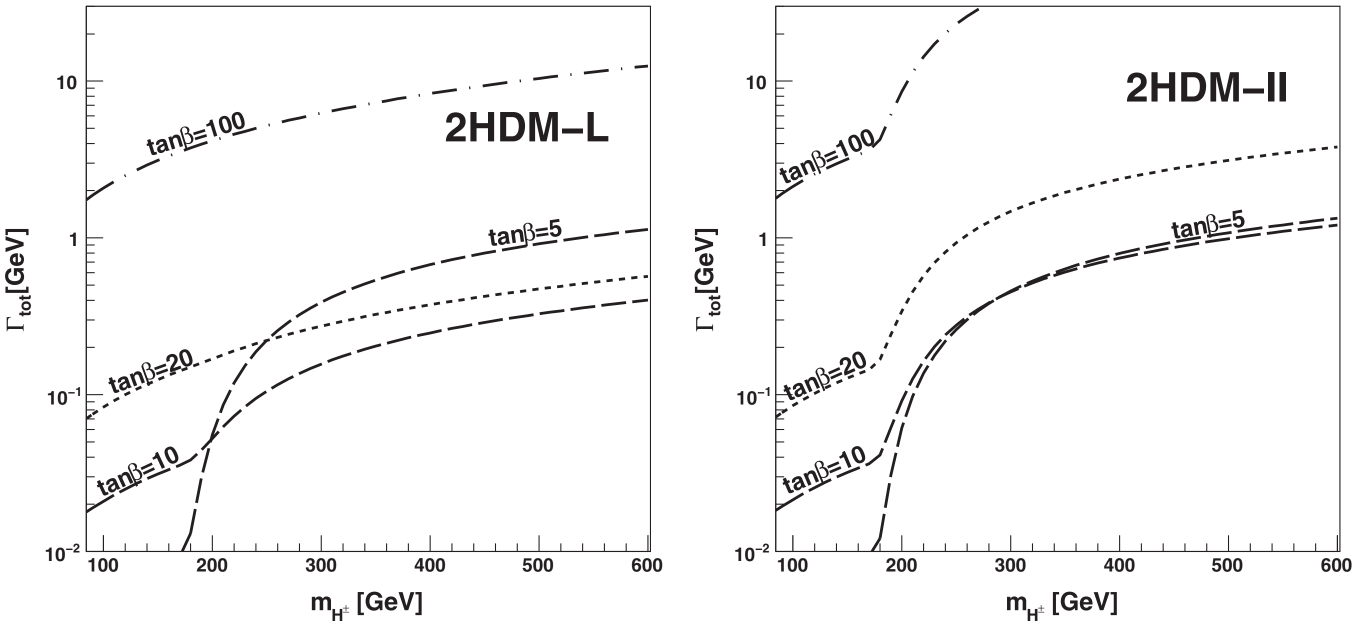

FIG. 7. Total width of $H^{\pm}$ as a function of $M_{H^{\pm}}$ for various values of $\tan\beta$.

For low $\tan\beta = 5$ (Fig. 3) the branching fractions of $H^{\pm}$ in the lepton-specific 2HDM are quite similar to those in the Type-II model, except that decays to bc and cs are suppressed. This is due to the $\cot\beta$ suppression in the Yukawa couplings of both up- and down-type quarks in this model. The tb mode remains dominant for $M_{H^{\pm}} \gtrsim (m_t + m_b)$ because $m_t \cot\beta$ is still large compared to $m_\tau \tan\beta$ for $\tan\beta = 5$.

As $\tan\beta$ increases, the suppression of the quark modes becomes more severe. For $\tan\beta = 20$, the branching fraction to $\tau\nu$ remains above 90% even for $M_{H^{\pm}}$ above the tb threshold. For higher $\tan\beta$ values, the leptonic decays dominate completely.

In Fig. 7 we show the total width of the charged Higgs as a function of $M_{H^{\pm}}$, for $\tan\beta = 5$, 10, 20, and 100. For comparison we again show the equivalent quantity for the Type-II model. Below the tb threshold, where decays in both models are dominated by the $\tau\nu$ final state, the total width of the charged Higgs is comparable in the two models.

Above the tb threshold, however, the different Yukawa coupling structure becomes obvious. At low $\tan\beta = 5$ the total width is dominated by tb and the tb threshold is obvious. As $\tan\beta$ increases, however, the total width first declines, increasing again only at large $\tan\beta$ where the $\tau\nu$ final state dominates and the tb threshold behavior disappears entirely. The total width of the charged Higgs in the lepton-specific 2HDM remains quite moderate, reaching $\sim$10 GeV only for large $\tan\beta \sim 100$ at $M_{H^{\pm}} = 600$ GeV. For lower $\tan\beta \sim 20$, the total width remains below 1 GeV in this mass range, much lower than for the Type-II model.

V. DISCUSSION AND CONCLUSIONS

The structure of the Yukawa couplings in the lepton-specific 2HDM poses a challenge for charged Higgs discovery at the LHC. The usual LHC discovery channels for the charged Higgs of the MSSM or other Type-II 2HDM involve production in association with a top quark [44,45] followed by decay to $\tau\nu$ or tb [46,47]. In the MSSM this production channel is particularly promising at large $\tan\beta$ because the production cross section due to Yukawa radiation off the bottom quark grows with $\tan^2\beta$. In the lepton-specific 2HDM, however, the cross section in this channel is proportional to $\cot^2\beta$ and thus heavily suppressed at large $\tan\beta$. For $M_{H^{\pm}}$ below the top quark mass, the decay $t \to H^+ b$ with $H^+ \to \tau\nu$ has also been studied for the LHC [47,48]. In the lepton-specific 2HDM the branching fraction for $t \to H^+ b$ is again suppressed by $\cot^2\beta$. We translate the 5σ charged Higgs discovery sensitivity quoted in Ref. [47] into the lepton-specific model by computing $\mathrm{BR}(t \to H^+ b)$ at tree level; we find the LHC discovery reach with 30 fb^{-1} to be $\tan\beta \lesssim 4.9$ (4.6, 2.4) for $M_{H^{\pm}} = 100$ (120, 150) GeV. Likewise, all other bottom-parton induced charged Higgs production processes in this model, such as H^+W^- associated production [49] and $b\bar{b} \to H^+H^-$ [50,51], as well as gluon fusion production of H^+H^- via a third-generation quark loop [51,52], are suppressed by powers of $\cot\beta$. Because of this, LHC searches for the charged Higgs in the lepton-specific 2HDM will have to rely on other production processes.

In Fig. 8 we show the cross sections for various charged Higgs production processes at the LHC. Production of

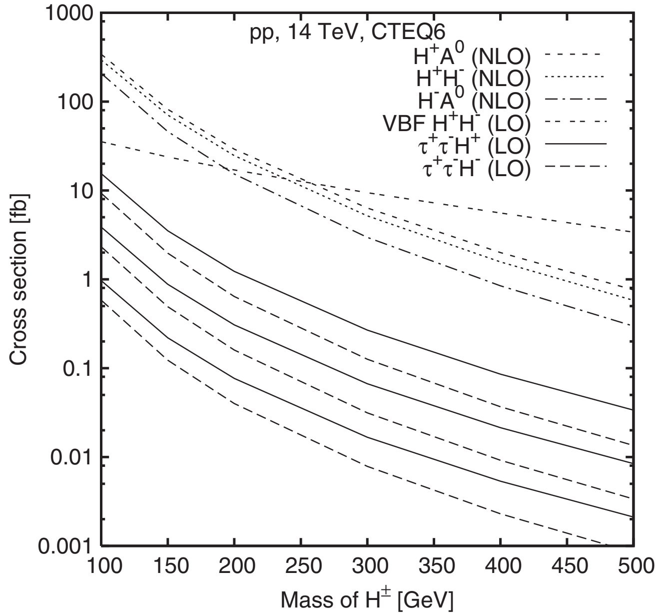

FIG. 8. Cross sections for charged Higgs production at the LHC (see text for details). The solid (dashed) lines show the cross sections for $\tau^+\tau^-H^+$ ($\tau^+\tau^-H^-$) production via Yukawa radiation for $\tan\beta = 200$, 100, and 50 from top to bottom. For $H^\pm A^0$ associated production we take $M_{A^0} = M_{H^\pm}$; the cross sections for $H^\pm H^0$ are identical to those for $H^\pm A^0$ when $M_{H^0} = M_{A^0}$ and the mixing angle in the CP-even sector is chosen so that the $W^+H^-h^0$ coupling vanishes. Leading-order (next-to-leading-order) cross sections are computed using CTEQ6L (CTEQ6M) [59] with renormalization and factorization scales set to M_Z ($M_{H^\pm}$).

charged Higgs pairs $q\bar{q} \to H^+H^-$ through an s-channel Z or photon [50,53] depends only on the charged Higgs mass once the SU(2) quantum numbers of the Higgs doublet are fixed. Similarly, associated production of $H^\pm$ and the CP-odd neutral Higgs boson A^0 through an s-channel W boson [54,55] depends only on the relevant scalar masses. Associated production of $H^\pm$ with a CP-even neutral Higgs boson (h^0 or H^0) depends on the masses involved as well as the mixing angle in the CP-even Higgs sector; if this mixing angle is chosen such that the $W^+H^-h^0$ coupling vanishes, the $H^\pm H^0$ cross section is equal to that for $H^\pm A^0$ for degenerate H^0 and A^0. We plot these cross sections in Fig. 8 including next-to-leading-order QCD corrections, computed using PROSPINO [56].[9]

Charged Higgs pair production due to vector boson fusion, $qq \to qqV^*V^* \to qqH^+H^-$ ($V = \gamma, Z, W^\pm$), was studied in detail in Ref. [57] in the MSSM. The cross section does not depend on the Yukawa structure of the model. It is smaller than that for $q\bar{q} \to H^+H^-$ for $M_{H^\pm} \lesssim 250$ GeV; however, the two forward jets provide a powerful selection tool against QCD backgrounds. Reference [57] studied signal and backgrounds in the decay channel $H^+H^- \to tb\tau\nu$ with the top quark decaying hadronically and found that the QCD top-pair background remains overwhelming. In the lepton-specific 2HDM, the dominant channel will be $H^+H^- \to \tau\nu\tau\nu$, which may provide a cleaner signature. We show this cross section in Fig. 8 (labeled *VBF* H^+H^-) as computed by MADGRAPH/MADEVENT [58].[10]

Finally, we consider the process $pp \to \tau^+\tau^-H^\pm$ in which the charged Higgs is radiated off one of the final-state τ leptons. The squared matrix element for $\bar{q}q' \to W^{+*} \to \tau^+\tau^-H^+$, neglecting external fermion masses, is given by

$$\sum_{\rm spins}|\mathcal{M}|^2 = g^4\left[\frac{gm_\tau}{\sqrt{2}M_W}\tan\beta\right]^2 \times \frac{4p_2\cdot k_1[2k_2\cdot k_3 p_1\cdot k_3 - M_{H^\pm}^2 p_1\cdot k_2]}{(q^2-M_W^2)^2(2k_2\cdot k_3 + M_{H^\pm}^2)^2}, \quad (41)$$

where p_1, p_2, k_1, k_2, and k_3 are the four-momenta of the incoming $\bar{q}$ and q', and outgoing τ^+, τ^-, and H^+, respectively, and $q = p_1 + p_2$. The cross section is proportional to $\tan^2\beta$; we show results for $\tan\beta = 50$, 100, and 200 in Fig. 8, computed using MADGRAPH/MADEVENT [58].

In summary, we studied the phenomenology of the charged Higgs boson in the lepton-specific 2HDM. We showed that the charged Higgs mass and $\tan\beta$ are constrained by existing data from direct searches at LEP and lepton flavor universality in τ decays; the former yields $M_{H^\pm} \geq 92.0$ GeV and the latter yields two allowed regions, $0.61\tan\beta$ GeV $\leq M_{H^\pm} \leq 0.73\tan\beta$ GeV or $M_{H^\pm} \geq 1.4\tan\beta$ GeV, excluding parameter space beyond the LEP-II bound for $\tan\beta \gtrsim 65$. Improvements on τ decay branching fractions at the proposed SuperB high-luminosity flavor factory would bring this reach down to $\tan\beta \gtrsim 30$. The B meson decays that are usually used to constrain the charged Higgs in the Type-II 2HDM provide no significant constraints in the lepton-specific model be-

[9] PROSPINO computes the cross sections for supersymmetric particle pair production at next-to-leading order. We note that the $pp \to H^+H^-$ cross section is identical to that for selectron pair production, $pp \to \tilde{e}_L\tilde{e}_L^*$, and that the $pp \to H^+A^0$ cross section is exactly half that of $pp \to \tilde{e}_L^*\tilde{\nu}_e$ for corresponding scalar masses. We eliminate the supersymmetric QCD corrections included in PROSPINO by taking the squark masses to be very heavy.

[10] We impose the following basic cuts on the jets in $pp \to jjH^+H^-$: $p_{Tj} \geq 20$ GeV, $\eta_j \leq 5$, $\Delta R_{jj} \geq 0.4$, and the dijet invariant mass $m_{jj} \geq 100$ GeV. Also, while their effects are small [57], neutral Higgs bosons enter as intermediate states in the vector boson fusion H^+H^- cross section calculation. For the relevant masses we choose $M_{A^0} = M_{H^0} = M_{H^\pm}$ and $M_{h^0} = 120$ GeV. We choose the mixing angle in the CP-even sector so that the $W^+H^-h^0$ coupling vanishes. The remaining free parameter is the $h^0H^+H^-$ coupling; we choose the coefficient of the Lagrangian term for $h^0H^+H^-$ to be equal to that for $h^0h^0h^0$ for the given h^0 mass.

cause the charged Higgs couplings to quarks are all proportional to $\cot\beta$.

We also studied the decay branching ratios of the charged Higgs in this model and showed that decays to quarks are heavily suppressed at large $\tan\beta$; in particular, the $t\bar{b}$ mode that typically dominates above threshold in the Type-II 2HDM falls below the 10% level for $\tan\beta \gtrsim 20$. Instead, $H^+ \rightarrow \tau\nu$ dominates at large $\tan\beta$ for all H^+ masses.

The suppression of the quark couplings to the charged Higgs at large $\tan\beta$ in this model poses a challenge for LHC discovery since it suppresses the tH^- associated production mode usually studied for the Type-II 2HDM. Instead, searches will have to rely on electroweak production of H^+H^- pairs or associated production of $H^\pm$ with a neutral Higgs boson. The cross section for associated production of $H^\pm\tau^+\tau^-$ via Yukawa radiation is small but it provides direct sensitivity to the τ Yukawa coupling.

ACKNOWLEDGMENTS

This work was supported by the Natural Sciences and Engineering Research Council of Canada. We thank D. Asner for helpful discussions on SuperB prospects.

Note added: As this paper was being completed, Ref. [11] appeared in which phenomenology of the same model was studied. Our results are largely consistent with theirs. For the indirect constraint from τ decays we choose to use the ratio of rates of $\tau \rightarrow \mu\nu\nu$ to $\tau \rightarrow e\nu\nu$ as opposed to the partial width $\Gamma(\tau \rightarrow \mu\nu\nu)$ for two reasons: (i) The experimental uncertainty on the ratio is smaller than that on the partial width, due to the non-negligible uncertainty in the τ lifetime; and (ii) the partial width $\Gamma(\tau \rightarrow \mu\nu\nu)$ receives potentially significant one-loop contributions from diagrams involving neutral Higgs bosons as pointed out in Ref. [24]; these effects cancel in the ratio of rates, allowing direct sensitivity to the charged Higgs sector.

[1] T. D. Lee, Phys. Rev. D **8**, 1226 (1973).
[2] P. Fayet, Nucl. Phys. **B78**, 14 (1974).
[3] R. D. Peccei and H. R. Quinn, Phys. Rev. Lett. **38**, 1440 (1977).
[4] P. Fayet and S. Ferrara, Phys. Rep. **32**, 249 (1977).
[5] H. Georgi, Hadronic J. **1**, 1227 (1978).
[6] H. E. Haber, G. L. Kane, and T. Sterling, Nucl. Phys. **B161**, 493 (1979).
[7] R. M. Barnett, G. Senjanovic, L. Wolfenstein, and D. Wyler, Phys. Lett. **136B**, 191 (1984).
[8] R. M. Barnett, G. Senjanovic, and D. Wyler, Phys. Rev. D **30**, 1529 (1984).
[9] Y. Grossman, Nucl. Phys. **B426**, 355 (1994).
[10] H. S. Goh, L. J. Hall, and P. Kumar, J. High Energy Phys. 05 (2009) 097.
[11] M. Aoki, S. Kanemura, K. Tsumura, and K. Yagyu, arXiv:0902.4665.
[12] S. Su and B. Thomas, Phys. Rev. D **79**, 095014 (2009).
[13] A. G. Akeroyd and W. J. Stirling, Nucl. Phys. **B447**, 3 (1995); A. G. Akeroyd, Phys. Lett. B **377**, 95 (1996); Nucl. Phys. **B544**, 557 (1999).
[14] A. G. Akeroyd, J. Phys. G **24**, 1983 (1998).
[15] B. Thomas, Phenomenology of a Lepton-Specific Higgs, talk presented at the Pheno 2008 Symposium, Madison, Wisconsin (2008), slides available from http://pheno.info/symposia/pheno08/.
[16] V. Barger, H. E. Logan, and G. Shaughnessy, arXiv:0902.0170.
[17] M. Aoki, S. Kanemura, and O. Seto, Phys. Rev. Lett. **102**, 051805 (2009).
[18] M. Misiak *et al.*, Phys. Rev. Lett. **98**, 022002 (2007).
[19] J. F. Gunion, H. E. Haber, G. L. Kane, and S. Dawson, *The Higgs Hunter's Guide* (Westview Press, Boulder, CO, 2000), SCIPP-89/13.
[20] LEP Higgs Working Group for Higgs boson searches, ALEPH, DELPHI, L3, and OPAL Collaborations, arXiv:hep-ex/0107031.
[21] G. Abbiendi *et al.* (OPAL Collaboration), Eur. Phys. J. C **32**, 453 (2004).
[22] P. Krawczyk and S. Pokorski, Phys. Rev. Lett. **60**, 182 (1988).
[23] W. Hollik and T. Sack, Phys. Lett. B **284**, 427 (1992).
[24] M. Krawczyk and D. Temes, Eur. Phys. J. C **44**, 435 (2005).
[25] J. M. Roney, Nucl. Phys. B, Proc. Suppl. **169**, 379 (2007).
[26] M. Bona *et al.*, arXiv:0709.0451.
[27] L. Michel, Proc. Phys. Soc. London Sect. A **63**, 514 (1950); C. Bouchiat and L. Michel, Phys. Rev. **106**, 170 (1957); T. Kinoshita and A. Sirlin, Phys. Rev. **108**, 844 (1957); **113**, 1652 (1959).
[28] W. Fetscher and H. J. Gerber, in S. Eidelman *et al.* (Particle Data Group), Phys. Lett. B **592**, 1 (2004).
[29] W. Fetscher and H. J. Gerber, in *Precision Tests of the Standard Electroweak Model* (World Scientific, Singapore, 1995), p. 657; Adv. Ser. Dir. High Energy Phys. **14**, 657 (1995).
[30] F. Scheck, Phys. Rep. **44**, 187 (1978).
[31] C. Amsler *et al.* (Particle Data Group), Phys. Lett. B **667**, 1 (2008).
[32] W. S. Hou, Phys. Rev. D **48**, 2342 (1993).
[33] A. G. Akeroyd, C. H. Chen, and S. Recksiegel, Phys. Rev. D **77**, 115018 (2008).
[34] A. Gray *et al.* (HPQCD Collaboration), Phys. Rev. Lett. **95**, 212001 (2005).
[35] E. Barberio *et al.* (Heavy Flavor Averaging Group), arXiv:0808.1297.
[36] E. Follana, C. T. H. Davies, G. P. Lepage, and J. Shigemitsu (HPQCD Collaboration and UKQCD Collaboration), Phys. Rev. Lett. **100**, 062002 (2008).
[37] B. A. Dobrescu and A. S. Kronfeld, Phys. Rev. Lett. **100**,

241802 (2008).

[38] Y. Grossman and Z. Ligeti, Phys. Lett. B **332**, 373 (1994).

[39] Y. Grossman, H. E. Haber, and Y. Nir, Phys. Lett. B **357**, 630 (1995).

[40] H. E. Logan and U. Nierste, Nucl. Phys. **B586**, 39 (2000); C. S. Huang, W. Liao, Q. S. Yan, and S. H. Zhu, Phys. Rev. D **63**, 114021 (2001); **64**, 059902(E) (2001); P. H. Chankowski and L. Slawianowska, Phys. Rev. D **63**, 054012 (2001); C. Bobeth, T. Ewerth, F. Kruger, and J. Urban, Phys. Rev. D **64**, 074014 (2001).

[41] J. L. Hewett, Phys. Rev. Lett. **70**, 1045 (1993).

[42] G. Yu, *et al.* (CDF Collaboration), CDF note Report No. 9322, 2008, available from http://www-cdf.fnal.gov; DØ Collaboration, DØ Note Report No. 5715-CONF, 2008, available from http://www-d0.fnal.gov.

[43] A. Djouadi, J. Kalinowski, and M. Spira, Comput. Phys. Commun. **108**, 56 (1998), code available from http://people.web.psi.ch/spira/hdecay/.

[44] R. M. Barnett, H. E. Haber, and D. E. Soper, Nucl. Phys. **B306**, 697 (1988); A. C. Bawa, C. S. Kim, and A. D. Martin, Z. Phys. C **47**, 75 (1990); V. D. Barger, R. J. N. Phillips, and D. P. Roy, Phys. Lett. B **324**, 236 (1994); F. Borzumati, J. L. Kneur, and N. Polonsky, Phys. Rev. D **60**, 115011 (1999).

[45] S. h. Zhu, Phys. Rev. D **67**, 075006 (2003); T. Plehn, Phys. Rev. D **67**, 014018 (2003); E. L. Berger, T. Han, J. Jiang, and T. Plehn, Phys. Rev. D **71**, 115012 (2005); J. Alwall and J. Rathsman, J. High Energy Phys. 12 (2004) 050; N. Kidonakis, J. High Energy Phys. 05 (2005) 011.

[46] G. L. Bayatian *et al.* (CMS Collaboration), CERN Report No. CERN-LHCC-2006-021, available from http://cdsweb.cern.ch.

[47] G. Aad *et al.* (The ATLAS Collaboration), arXiv:0901.0512.

[48] M. Baarmand, M. Hashemi, and A. Nikitenko, J. Phys. G **32**, N21 (2006).

[49] D. A. Dicus, J. L. Hewett, C. Kao, and T. G. Rizzo, Phys. Rev. D **40**, 787 (1989); A. A. Barrientos Bendezu and B. A. Kniehl, Phys. Rev. D **59**, 015009 (1998).

[50] A. Alves and T. Plehn, Phys. Rev. D **71**, 115014 (2005).

[51] A. A. Barrientos Bendezu and B. A. Kniehl, Nucl. Phys. **B568**, 305 (2000).

[52] S. S. D. Willenbrock, Phys. Rev. D **35**, 173 (1987); A. Krause, T. Plehn, M. Spira, and P. M. Zerwas, Nucl. Phys. **B519**, 85 (1998); O. Brein and W. Hollik, Eur. Phys. J. C **13**, 175 (2000).

[53] E. Eichten, I. Hinchliffe, K. D. Lane, and C. Quigg, Rev. Mod. Phys. **56**, 579 (1984); **58**, 1065 (1986).

[54] S. Kanemura and C. P. Yuan, Phys. Lett. B **530**, 188 (2002).

[55] Q. H. Cao, S. Kanemura, and C. P. Yuan, Phys. Rev. D **69**, 075008 (2004).

[56] W. Beenakker, M. Klasen, M. Kramer, T. Plehn, M. Spira, and P. M. Zerwas, Phys. Rev. Lett. **83**, 3780 (1999); **100**, 029901 (2008).

[57] S. Moretti, J. Phys. G **28**, 2567 (2002).

[58] J. Alwall *et al.*, J. High Energy Phys. 09 (2007) 028.

[59] J. Pumplin, D. R. Stump, J. Huston, H. L. Lai, P. M. Nadolsky, and W. K. Tung, J. High Energy Phys. 07 (2002) 012.